

Chain-Scission-Induced Intercalation as a Facile Route to Polymer Nanocomposites**

By David J. Frankowski, Saad A. Khan, and Richard J. Spontak*

Polymer/clay nanocomposites (NCs) prepared using melt intercalation must be properly formulated and processed to achieve intercalation or exfoliation. Organically modified layered silicates (OMLSs) are often used to permit polymer intercalation and thereby separate the silicate platelets. Prior modeling efforts^[1] suggest that high-molecular-weight (HMW) polymers tend to yield immiscible NCs unlike their low-molecular-weight (LMW) analogs, which commonly result in exfoliated or intercalated NCs. Although formulations containing LMW polar additives (e.g., maleic anhydride copolymers) have succeeded in producing at least partially exfoliated rather than immiscible NCs,^[2–4] a need persists for simpler HMW formulations in order to expedite industrial scale-up.

The present study examines blends composed of HMW polystyrene (PS) and an OMLS that remains largely immiscible when annealed under an inert N₂ atmosphere with little or no shear. Controlled thermal-oxidative chain scission of the HMW PS in an O₂-rich environment promotes intercalation of short PS chains within the OMLS, thereby expanding and disordering the platelets as an intercalated NC develops. This scission-induced intercalation mechanism ensures that the resultant NC is in a thermodynamically stable state unlike NCs prepared using in situ polymerization, which may deintercalate during further processing.^[5,6] Moreover, scission intercalation may be used as a general means by which to promote intercalation or possibly exfoliation in previously reported^[4,7,8] immiscible NCs.

Polymeric NCs containing clay have become an increasingly important topic in the development of lightweight,^[9–12] tough,^[13–19] and impermeable^[18–21] materials since the Toyota research laboratories polymerized nylon-6 in the presence of sodium montmorillonite (Na-MMT) for automotive applications in the late 1980s.^[22] In situ polymerization has enjoyed the most success in producing exfoliated NCs wherein individual clay platelets are uniformly dispersed in a polymeric ma-

trix, because the polymer chains can grow within the silicate galleries. Another NC-fabrication strategy is solution intercalation,^[23] in which polymer, solvent, and clay are mixed together. In this case, confinement of polymer chains upon diffusion into the silicate galleries is compensated for by the entropic gain caused by desorbed solvent molecules. Both in situ polymerization and solution intercalation typically require relatively large quantities of organic solvent, whereas melt intercalation^[24] relies on annealing above the glass-transition (T_g) or melting (T_m) temperature of the polymer matrix under static or shear conditions. Melt intercalation constitutes an environmentally benign and commercially feasible process that successfully yields intercalated or exfoliated NCs from more polymer–clay pairs than either in situ polymerization or solution intercalation.

Giannelis and co-workers^[24–26] have previously demonstrated that sieved PS powder can intercalate into fluorohectorite under static annealing in an inert N₂ atmosphere at 180 °C and below. At molecular weights comparable to that of the PS used in the present study (weight-average molecular weight, M_w , 330 kg mol⁻¹), noticeable intercalation requires approximately six hours.^[26] This result reflects their observation that the diffusion of PS into the silicate galleries under quiescent conditions becomes increasingly difficult with increasing chain length. Complementary studies have shown that twin-screw extrusion of HMW PS and OMLS with optimized screw profiles can overcome diffusion limits associated with static annealing at high temperatures, as well as circumvent undesirable dispersion issues.^[25,27–30] Under routine operating conditions, however, we expect sufficient concentrations of O₂ to be present^[31] for thermal-oxidative chain scission to occur. Indeed, an increase in temperature^[32] or addition of clay^[33] have been independently found to increase the rate of PS chain scission in the melt. Although most studies do not report M_w for the polymer after extrusion, we propose that the sequential chain-scission–intercalation mechanism described below may be at least partially responsible for the intercalation of polymer into OMLSs and the corresponding formation of NCs from HMW PS.

Our system was designed to be commercially relevant as resins are usually obtained in pellet form and the screw of an extruder may not always be optimized for clay intercalation because of multiple products being run on a common manufacturing line. Single-screw extrusion of HMW PS and Cloisite 15A OMLS at a melt temperature of 185 °C yielded an immiscible NC according to X-ray diffractometry (XRD). As discussed later, extruded PS/OMLS exhibited a principal peak

[*] Prof. R. J. Spontak, Dr. D. J. Frankowski,^[†] Prof. S. A. Khan
Department of Chemical & Biomolecular Engineering
North Carolina State University, Raleigh, NC 27695 (USA)
E-mail: rich_spontak@ncsu.edu

Prof. R. J. Spontak
Department of Materials Science & Engineering
North Carolina State University, Raleigh, NC 27695 (USA)

[†] Current address: Dow Building Solutions Research & Development,
Dow Chemical Co., Midland, MI 48674, USA.

[**] This study was supported by the STC Program of the National Science Foundation under Agreement No. CHE-9876674.

at the same scattering position as that of the pristine clay, indicating that the d -spacings of the virgin clay and composite were identical. To obtain structural data free of orientation artifacts, powdered samples were loaded into capillaries mounted on a rotating goniometer for measurement in transmission mode. Size exclusion chromatography (SEC) confirmed that the M_w of PS in the NC was reduced from 330 to 263 kg mol⁻¹ upon extrusion. Although a forthcoming study will detail the intricate molecular-level changes in PS upon static annealing of extruded PS/OMLS under different conditions, suffice it to say, at the present time, that annealing the extruded NC in a rheometer operated in an O₂-rich environment (air) below 220 °C subsequently resulted in slight chain scission and negligible intercalation according to ex situ SEC and XRD analyses, respectively. The net effect of these two molecular-level processes on mechanical property evolution was monitored in situ here as a function of post-extrusion annealing time (t) using dynamic oscillatory shear in the linear viscoelastic regime.

Figure 1a confirms that the storage modulus (G') decreased slightly at 170 °C, which is consistent with chain degradation

and a reduction in M_w . At 220 °C, however, the decrease in G' was less pronounced, suggesting that the extent of chain scission incurred was offset by limited OMLS intercalation. It is important to note that the moduli for neat PS annealed under identical conditions systematically decreased with time solely because of chain scission. Although we recognize that the alkyl ammonium cation in the silicate will most likely begin to degrade under these thermal conditions and reduce the effective PS diffusion coefficient into the OMLS, annealing under N₂ below 220 °C did not promote noticeable evidence of intercalation.

Figure 1a further reveals that annealing the NCs in an O₂-rich atmosphere at 250 °C yielded a remarkable increase in G' , whereas the response of neat PS to such annealing in an O₂-rich environment was a continued decrease in G' . Under these conditions, SEC corroborates that neat PS and the PS NCs undergo chain scission and little, if any, cross-linking, which would also serve to increase G' . Although other mechanisms could be responsible for the observed increase in G' , this signature, in conjunction with corresponding SEC and XRD data, strongly suggests that OMLS intercalation was at least partially responsible for the modulus increase. That is, conditions favoring this increase in G' promoted the formation of LMW chains, discerned by using SEC, and a concurrent increase in clay d -spacing, measured by using XRD. Conversely, minimal changes in elastic modulus were accompanied by modest PS M_w changes and diffraction patterns quantitatively reminiscent of the pristine clay. The PS NC annealed under N₂ at 250 °C showed a less profound temporal increase in G' compared to annealing in air. A reduction in the concentration of O₂ (introduced upon loading the specimen into the environmental testing chamber of the rheometer) slowed chain scission, as confirmed by SEC, which in turn diminished the rate of intercalation, as reflected by the lower slope of $G'(t)$ in Figure 1a. Doubling the N₂ pressure and purge rate (from 138 to 276 kPa and 0.6 to 1.2 m³ h⁻¹, respectively) reduced the propensity for further chain scission (and, thus, intercalation as well), in which case G' did not increase to a meaningful extent (Fig. 1b). Switching back to an O₂-rich environment caused G' to increase at a rate similar to that in Figure 1a. When the atmosphere was changed back to N₂, the likelihood of chain scission was drastically reduced and intercalation again slowed considerably, as indicated by the nearly constant $G'(t)$ in Figure 1b.

Scattering patterns of the PS NCs acquired after different annealing times in an O₂-rich atmosphere at 250 °C are presented in Figure 2 and demonstrate that both the platelet d -spacing and full width at half-maximum (FWHM) derived from the principal scattering peak of the OMLSs in the vicinity of an angle (2θ) of 2.6–2.8° increase with increasing t . The time-dependent increase in disorder of the platelets, signified by the measured increase in the FWHM, strengthened the clay network that contributed, along with platelet separation, to the increase in G' evident in Figure 1a. Using the scattering data, the number of clay platelets per particle was estimated from the Scherrer equation^[34] to decrease from approximately

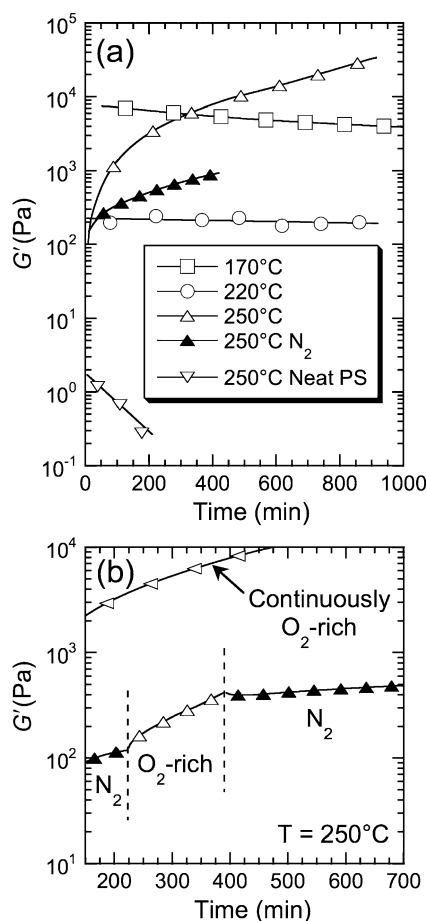


Figure 1. Changes in G' for NCs with 7 wt% clay when annealed in O₂-rich (unfilled symbols) and N₂ (filled symbols) environments between 170 and 250 °C. The N₂ pressure and purge rate in (b) are double that in (a). Dynamic oscillatory shear at a frequency of 0.1 rad s⁻¹ acquires data points every ca. 2.5 min, but not all points are shown for clarity. The solid lines serve to connect the data.

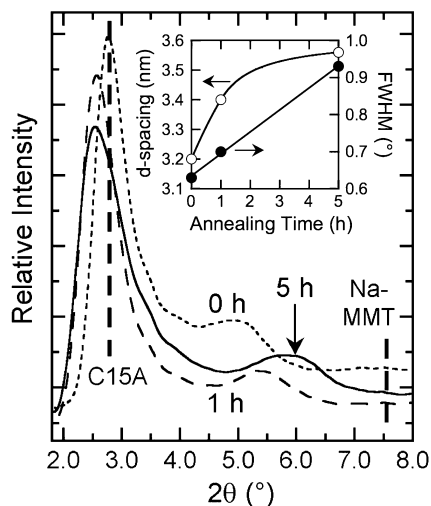


Figure 2. XRD patterns for NCs with 17 wt% clay annealed in an O₂-rich environment at 250 °C for different times (labeled). The vertical dashed lines indicate the peak positions for pristine Cloisite 15A and Na-MMT. The inset shows the increases in the *d*-spacing (○) and FWHM (●) corresponding to the reflex at ca. 2.8° 2θ with annealing time. In the inset, the lines serve as a guide to the eye.

5 to 4 after 5 h of annealing. Values of the *d*-spacing and FWHM derived from the XRD patterns displayed in Figure 2 are provided as a function of *t* in the inset. Note that thermal annealing of the OMLS in air also degrades the alkyl ammonium cation, resulting in unintercalated clay with a substantially reduced *d*-spacing (peaks between 5.0 and 6.0° 2θ). An increase in annealing time from 1 to 5 h shifted this peak to higher 2θ, indicating greater degradation of the cation and further collapse of the platelets. The *d*-spacing measured for Na-MMT is included for reference in Figure 2.

Ex situ XRD of neat clay annealed at high temperatures likewise showed peak growth at, and a shift to, higher 2θ values (data not shown). Desorption of alkyl chains resulting from cation degradation provides an entropic driving force to lower the system free energy, because desorbed chains gain translational freedom and reduce the packing density at the silicate surface. A delicate balance between alkyl chain length and packing density exists such that intermediate values of both are typically required for intercalation.^[26] At high packing densities, the alkyl chains adopt a rigid paraffinic arrangement and cannot gain conformational freedom as the platelets separate, resulting in immiscible NCs.^[26,35,36]

Prior studies^[25,26] report intercalation for HMW PS during static annealing under N₂ at 180 °C and below, whereas the present system did not show evidence of intercalation (inferred from the lack of increases in *G'* and *d*-spacing) under comparable annealing conditions. It must be recognized, however, that the OMLS used in our study is chemically dissimilar from that previously used (organically

modified fluorohectorite), and thus the alkyl length and packing density, as well as PS wettability,^[37–39] differ. In the present system, PS chain scission is required to promote OMLS intercalation, which is consistent with model predictions indicating that intercalation by LMW chains is thermodynamically preferred over HMW chains.^[1] A schematic illustration of the scission–intercalation mechanism proposed here is provided in Figure 3. After the HMW PS and OMLS (Fig. 3a) were mixed in a single-screw extruder, they formed an immiscible NC wherein large PS chains extended along the edges of, and “bridged,” the silicate galleries. This arrangement (Fig. 3b) effectively thwarted intercalation. Simulation,^[40] theoretical,^[41] and experimental^[42] studies confirm that such bridging, which may develop in the absence of specific interactions,^[43] is sufficient to prevent intercalation. Although the *d*-spacing of the OMLS remained unchanged after extrusion, the FWHM decreased, indicating that interparticle fusion occurred, caused by silicate–silicate attraction. Such aggregation severely limits intercalation kinetics.^[24,25,30] For instance, the extents to which PS (*M*_w = 30 kg mol^{−1}) intercalates into fluorohectorite after annealing in air at 170 °C for 40 min have been reported^[25] as ca. 100 % and 55 % for particle sizes < 100 μm and > 200 μm, respectively.

Annealing the immiscible NC at low temperatures or in an inert atmosphere (N₂ or vacuum) had no discernible effect on morphology, although SEC and rheology revealed that limited, but apparently insufficient, chain scission occurs. Annealing at high temperatures increased the extent of chain scission, producing chains with *M*_w < 60 kg mol^{−1}. These short PS chains could diffuse between large PS chains, as well as between the silicate layers (Fig. 3c). Degradation is anticipated to occur preferentially along the periphery of the platelets because OMLSs are known^[33] to accelerate PS chain scission.

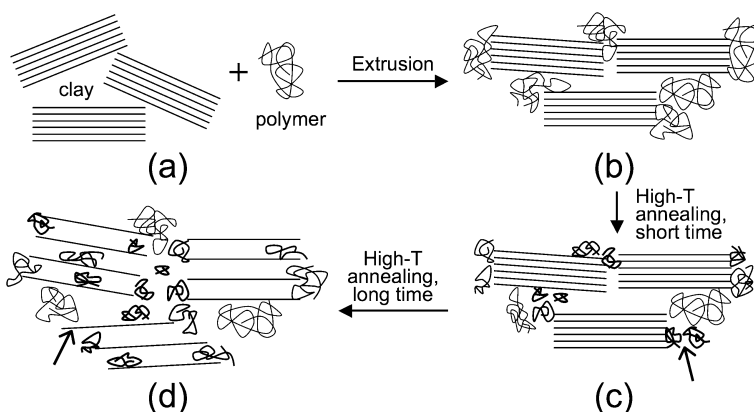


Figure 3. A schematic diagram depicting the evolution of NC morphology upon extrusion and subsequent annealing. In (a), clay aggregates and polymer were extruded to yield (b) agglomerates with polymer chains bridging potential intercalation sites. Low-temperature annealing or annealing in an inert atmosphere resulted in negligible changes from (b), whereas high-temperature annealing in the presence of O₂ resulted in (c) chain scission of the bridging polymers and diffusion of short chains past bridging chains (indicated by the arrow). At long times (d), short PS chains generated by scission intercalated into the interlayers and increased the *d*-spacing and disorder of the platelets, the latter augmented by silicate-sheet sliding as indicated by the arrow.

After long times (Fig. 3d), short PS chains generated from chain scission occupied the OMLS galleries, forcing the platelets apart and increasing the d -spacing. Largely intact PS chains remained in the melt pool surrounding the OMLS particles and either migrated to the periphery of the clay platelets, where they, too, could undergo scission, or diffused directly into the galleries if the d -spacing was sufficiently large. In either case, the d -spacing and disorder of the platelets continued to increase. Intercalation of PS chains, especially large ones, can promote sheet sliding, which exposes platelet surface area and further increases the FWHM of the principal scattering peak, thereby indicating enhanced disorder. Under continued shear, PS-induced sheet sliding can subsequently result in the formation of elongated, intercalated OMLS particles, or even limited OMLS exfoliation, both of which would serve to increase G' .

Extrusion of OMLS with LMW PS ($M_w = 45 \text{ kg mol}^{-1}$) was likewise performed to confirm that short chains could intercalate into the clay galleries under nondegrading conditions. Rheology and XRD confirmed the formation of an intercalated NC after extrusion, as well as enhanced intercalation upon annealing at relatively low temperatures. These results will be reported in detail elsewhere. Although addition of LMW PS to HMW PS can have a similar effect as depicted in Figure 3, the scission–intercalation mechanism enjoys two strategic advantages. Firstly, the formulation is less complicated and so industrial scale-up is facile. Secondly, the LMW chains are, for the most part, present where they are needed most. Adding LMW PS can deleteriously influence mechanical properties if they locate in the PS matrix. As PS chain scission is expected to proceed near the OMLS edges, the short PS chains produced in this fashion can diffuse into the clay galleries, minimizing the concentration of LMW PS in the bulk. The scission–intercalation mechanism proposed here, wherein LMW chains are first produced by thermal-oxidative chain scission and then intercalated into the OMLS particles, suggests that PS chain scission can be spatially tunable, using the clay particles as a catalyst and thus minimizing the fraction of undesirable LMW PS in the bulk where they would have a negative impact on mechanical properties. As annealing NCs in an inert environment dramatically reduced the extents of chain scission and intercalation, we further provide direct evidence (in Fig. 1b) that thermal-oxidative scission and, thus, intercalation can effectively be switched “on” and “off” with a minimal transition time (ca. 1 min) via judicious choice of annealing atmosphere. This strategy strongly suggests that other process routes, such as high-energy milling^[44] or solid-state shear compounding,^[45] that are likewise capable of inducing localized chain scission could also be used to promote intercalation or, ultimately, exfoliation in polymer/clay NCs.

Experimental

Polystyrene 1300 with a melt index of 3.5 g/10 min (American Society for Testing and Materials (ASTM) D1238 at 200 °C and with 5 kg) was kindly supplied in pellet form by Nova Chemicals (Calgary,

Alberta, Canada), and the OMLS was Cloisite 15A, a MMT modified with a quaternary ammonium salt (dimethyl dihydrogenated tallow), acquired from Southern Clay Products (Gonzales, TX). The OMLS was dried overnight under vacuum prior to compounding. Alkanox 240, an organophosphite antioxidant, was provided by Great Lakes Chemical (West Lafayette, IN), and prepurified industrial-grade N_2 (99.99% purity) was obtained from National Welders Supply Co. (Charlotte, NC). High-performance liquid chromatography (HPLC) grade tetrahydrofuran (THF) from Acros Organics (Morris Plains, NJ) was used as-received for SEC. Formulations with clay concentrations of 7 or 17 wt % were prepared by manually dry-blending PS pellets, clay, and 0.6 wt % stabilizer in glass jars for 5 min prior to addition to the hopper mounted on a 3/4" single-screw extruder (Wayne Machine & Die Co., Wayne, NJ) with length/diameter = 30/1, and with a Saxton mixing section at its end. Samples were extruded at 50 rpm through the bore possessing a temperature profile (in °C) of 140/175/180/185. The adapter and die temperatures were maintained at 185 °C. Discs for rheometry were melt-pressed at 175 °C and 5 MPa in circular molds of varying thickness and either 8, 10, or 25 mm diameter. The circular molds were quickly removed from the platens and quenched in chilled water (10–20 °C).

Dynamic oscillatory shear using parallel plates was conducted on either an Advanced Rheometric Expansion System (ARES) operated in strain-controlled mode or an AR2000 in stress-controlled mode. Both units are from TA Instruments (New Castle, DE). All samples were vacuum-treated at least overnight prior to testing. The linear viscoelastic limit for each formulation was identified by performing a strain or stress sweep at a fixed frequency. Temporal experiments, conducted at a frequency of 0.1 rad s^{-1} with data points collected every 2.5 min, were performed at least in duplicate to confirm trends, and both rheometers yielded comparable G' values. The XRD patterns were acquired on an Inel XRG 3000 diffractometer (Artenay, France) with $\text{CuK}\alpha$ radiation (wavelength $\lambda = 0.15405 \text{ nm}$) at 35 kV and 30 mA. Samples for XRD were tested in either reflection mode using the Bragg-Brentano parafocusing geometry (powders and films) at an incidence angle $< 5^\circ$ or using transmission mode by loading powder into 0.3–0.7 mm glass capillary tubes. Data were collected on a stationary detector. Molecular weights were measured at 25 °C using a DAWN multiangle light scattering (MALS) instrument in conjunction with an Optilab interferometric refractometer from Wyatt Technology Corp. (Santa Barbara, CA) and a Waters 2950 HPLC injection system from Waters Corp. (Milford, MA). Most SEC analyses were performed at 0.5 mL min^{-1} in THF with Styragel HR4 and HR4E columns. Select specimens were further examined with a Waters 2695 HPLC unit outfitted with μ Styragel columns (pore sizes 10^4 , 10^3 , and 10^2 nm) and operated with THF at 1.0 mL min^{-1} using a Waters 410 refractometer and a MALS detector with a universal calibration curve.

Received: April 11, 2006

Revised: November 17, 2006

Published online: March 15, 2007

- [1] Y. Lyatskaya, A. C. Balazs, *Macromolecules* **1998**, *31*, 6676.
- [2] M. Kawasumi, N. M. Kato, A. Usuki, A. Okada, *Macromolecules* **1997**, *30*, 6333.
- [3] M. J. Solomon, A. S. Almusallam, K. F. Seefeldt, A. Somwangthanoj, P. Varadan, *Macromolecules* **2001**, *34*, 1864.
- [4] G. Galgali, C. Ramesh, A. Lele, *Macromolecules* **2001**, *34*, 852.
- [5] A. Tabtiang, S. Lumlong, R. A. Venables, *Polym.-Plast. Technol. Eng.* **2000**, *39*, 293.
- [6] X. Y. Huang, W. J. Brittain, *Macromolecules* **2001**, *34*, 3255.
- [7] Y. T. Lim, O. O. Park, *Macromol. Rapid Commun.* **2000**, *21*, 231.
- [8] M. Y. Gelfer, H. H. Song, L. Z. Liu, B. S. Hsiao, B. Chu, M. Rafailovich, M. Y. Si, V. Zaitsev, *J. Polym. Sci., Part B: Polym. Phys.* **2002**, *41*, 44.
- [9] B. N. Jang, D. Y. Wang, C. A. Wilkie, *Macromolecules* **2005**, *38*, 6533.

- [10] M. R. Bockstaller, R. A. Mickiewicz, E. L. Thomas, *Adv. Mater.* **2005**, *17*, 1331.
- [11] L. Xu, S. Reeder, M. Thopasridharan, J. X. Ren, D. A. Shipp, R. Krishnamoorti, *Nanotechnology* **2005**, *16*, S514.
- [12] W. B. Zha, S. Choi, K. M. Lee, C. D. Han, *Macromolecules* **2005**, *38*, 8418.
- [13] H. A. Stretz, D. R. Paul, R. Li, H. Keskkula, P. E. Cassidy, *Polymer* **2005**, *46*, 2621.
- [14] D. Shah, P. Maiti, D. D. Jiang, C. A. Batt, E. P. Giannelis, *Adv. Mater.* **2005**, *17*, 525.
- [15] Y. H. Ha, Y. Kwon, T. Breiner, E. P. Chan, T. Tzianetopoulou, R. E. Cohen, M. C. Boyce, E. L. Thomas, *Macromolecules* **2005**, *38*, 5170.
- [16] C. K. Lam, K. T. Lau, H. Y. Cheung, H. Y. Ling, *Mater. Lett.* **2005**, *59*, 1369.
- [17] J. I. Weon, H. J. Sue, *Polymer* **2005**, *46*, 6325.
- [18] T. Y. Tsai, C. H. Li, C. H. Chang, W. H. Cheng, C. L. Hwang, R. J. Wu, *Adv. Mater.* **2005**, *17*, 1769.
- [19] X. Cao, L. J. Lee, T. Widya, C. Macosko, *Polymer* **2005**, *46*, 775.
- [20] M. M. Malwitz, A. Dundigalla, V. Ferreira, P. D. Butler, M. C. Henk, G. Schmidt, *Phys. Chem. Chem. Phys.* **2004**, *6*, 2977.
- [21] C. S. Lu, Y. W. Mai, *Phys. Rev. Lett.* **2005**, *95*.
- [22] A. Usuki, Y. Kojima, M. Kawasumi, A. Okada, Y. Fukushima, T. Kurauchi, O. Kamigaito, *J. Mater. Res.* **1993**, *8*, 1179.
- [23] T. Lan, P. D. Kaviratna, T. J. Pinnavaia, *Chem. Mater.* **1994**, *6*, 573.
- [24] R. A. Vaia, H. Ishii, E. P. Giannelis, *Chem. Mater.* **1993**, *5*, 1694.
- [25] R. A. Vaia, K. D. Jandt, E. J. Kramer, E. P. Giannelis, *Macromolecules* **1995**, *28*, 8080.
- [26] R. A. Vaia, E. P. Giannelis, *Macromolecules* **1997**, *30*, 8000.
- [27] B. Hoffmann, C. Dietrich, R. Thomann, C. Friedrich, R. Mülhaupt, *Macromol. Rapid Commun.* **2000**, *21*, 57.
- [28] S. Tanoue, L. A. Utracki, A. Garcia-Rejon, J. Tatibouët, K. C. Cole, M. R. Kamal, *Polym. Eng. Sci.* **2004**, *44*, 1046.
- [29] D. Z. Chen, H. Y. Yang, P. S. He, W. A. Zhang, *Compos. Sci. Technol.* **2005**, *65*, 1593.
- [30] Y. Q. Li, H. Ishida, *Macromolecules* **2005**, *38*, 6513.
- [31] N. C. Billingham, P. D. Calvert, in *Degradation and Stabilisation of Polyolefins* (Ed: N. S. Allen), Elsevier, New York **1983**, Ch. 1.
- [32] H. H. G. Jellinek, *J. Polym. Sci.* **1948**, *3*, 850.
- [33] J. W. Gilman, C. L. Jackson, A. B. Morgan, R. Harris, E. Manias, E. P. Giannelis, M. Wuthenow, D. Hilton, S. H. Phillips, *Chem. Mater.* **2000**, *12*, 1866.
- [34] B. D. Cullity, S. R. Stock, *Elements of X-ray Diffraction*, 3rd ed., Prentice Hall, Upper Saddle River, NJ **2001**, p. 664.
- [35] F. L. Beyer, N. C. B. Tan, A. Dasgupta, M. E. Galvin, *Chem. Mater.* **2002**, *14*, 2983.
- [36] S. Limpanart, S. Khunthon, P. Taepaiboon, P. Supaphol, T. Srikhirin, W. Udomkichidecha, Y. Boontongkong, *Mater. Lett.* **2005**, *59*, 2292.
- [37] F. W. Starr, T. B. Schröder, S. C. Glotzer, *Phys. Rev. E* **2001**, *6402*.
- [38] A. Bansal, H. C. Yang, C. Z. Li, K. W. Cho, B. C. Benicewicz, S. K. Kumar, L. S. Schadler, *Nat. Mater.* **2005**, *4*, 693.
- [39] C. J. Ellison, M. K. Mundra, J. M. Torkelson, *Macromolecules* **2005**, *38*, 1767.
- [40] J. Y. Lee, A. R. C. Baljon, R. F. Loring, *J. Chem. Phys.* **1999**, *111*, 9754.
- [41] A. C. Balazs, C. Singh, E. Zhulina, *Macromolecules* **1998**, *31*, 8370.
- [42] J. Swenson, M. V. Smalley, H. L. M. Hatharasinghe, *Phys. Rev. Lett.* **1998**, *81*, 5840.
- [43] M. Vacatello, *Macromolecules* **2001**, *34*, 1946.
- [44] A. P. Smith, J. S. Shay, R. J. Spontak, C. M. Balik, H. Ade, S. D. Smith, C. C. Koch, *Polymer* **2000**, *41*, 6271.
- [45] W. G. Shao, Q. Wang, Y. H. Chen, Y. Gu, *Mater. Manuf. Processes* **2006**, *21*, 173.